

---

## Observation of gamma-rays greater than 10 TeV from Markarian 421

---

Kimihiko Okumura

*Institute for Cosmic Ray Research, University of Tokyo, 5-1-5 Kashiwa-no-Ha,  
Kashiwa City, Chiba 277-8582, Japan*

for CANGAROO collaboration

---

### Abstract

We have observed Markarian 421 during an extraordinarily high state in January and March 2001 with the CANGAROO-II imaging Cherenkov telescope. From 14 hours observations at a large zenith angle of  $\sim 70^\circ$ , a signal of  $298 \pm 52$  gamma-ray-like events was detected at  $E > 10$  TeV with  $5.7 \sigma$  significance. Under the assumption of power-law spectrum, we derived a steep energy spectrum of photon index  $\sim 4.0$ , and supports the evidence for a cutoff in the spectrum of Markarian 421. However, the  $4 \sigma$  excess at energies greater than 20 TeV in our data favors a cutoff energy of  $\sim 8$  TeV, at the upper end of the range previously reported from measurements at TeV energies.

### 1. Introduction

Markarian 421 (Mrk 421, J1104+3812) is a nearby BL Lacertae object ( $z = 0.031$ ) and was the first extragalactic TeV gamma-ray source discovered [14]. Mrk 421 became active in 2000 and 2001, especially at the beginning of 2001 [4]. During this period, northern hemisphere observers measured the energy spectrum with good statistics in the region from several hundred GeV to  $\sim 10$  TeV and reported cutoffs at 3–6 TeV [3] [10]. The cutoff energy is consistent with, or slightly smaller than, that measured for Mrk 501 during its flaring state in 1997 [1] [2]. As Mrk 501 has a similar redshift ( $z = 0.034$ ) to Mrk 421, this suggests the cutoffs may be due to absorption of TeV gamma-rays, which is caused by photon-photon interactions with the inter-galactic infrared background [8] [7] [18].

### 2. Observation and analysis

Mrk 421 was observed for ten nights in early 2001; January 24, 26, 27, 30, 31 and February 1, and March 1–4 (all dates in UT), when the source was extremely active. Approximately two hours observations were made per night, at

zenith angles of  $69^{\circ}.3$ – $71^{\circ}.5$ . After rejecting inefficient data affected by clouds, 14.34 hours ON source data and 16.65 hours OFF source data remain.

Large zenith angle observations are well-suited to searching for gamma-ray signals at higher energies, as a much larger effective area can be achieved compared to observations near the zenith [17] [19], though with a higher energy threshold. From Monte Carlo simulations [13] [5], an effective area of  $\sim 5 \times 10^9 \text{ cm}^2$  at  $E = 20 \text{ TeV}$  was estimated for observations at  $70^\circ$ , with the area increasing to  $\sim 10^{10} \text{ cm}^2$  for higher energies. A threshold energy (where the gamma-ray detection rate is maximized) of  $\sim 11 \text{ TeV}$  was derived for a  $E^{-3.0}$  spectrum. This is an increase by a factor of  $\sim 30$  in comparison with observations near zenith.

The selection of the gamma-ray events is based on the parameterization of the elongated shape of the Cherenkov light image using the standard parameters: *width*, *length* (shape), *distance* (location), *asymmetry* (direction), and *alpha* (orientation angle) [9] [15] [16]. Instead of the conventional parameterization cuts, we adopted the Likelihood method [5] [6], which has a higher efficiency of gamma-ray discrimination than the conventional parameterization technique. The likelihood method uses a single parameter,  $R_{prob} = Prob(\gamma) / [Prob(\gamma) + Prob(B.G.)]$ , where  $Prob(\gamma)$  and  $Prob(B.G.)$  are the probabilities for the event having been initiated by a gamma-ray from the source or a background event, respectively. They are the products of individual probabilities for *width*, *length*, and *asymmetry*, which are derived from the probability density functions, including the energy dependence. These functions were obtained using gamma-ray simulations for the signal and the observed OFF source events for the background. We adopted a relatively loose cut of  $R_{prob} > 0.4$  with an additional requirement of  $0^\circ.2 < distance < 1^\circ.1$ . With these cuts and a further cut excluding events with  $alpha \geq 20^\circ$ , 86 % of background events are rejected while 63 % of gamma-ray events are expected to be retained.

### 3. Results

The resulting event distribution of *alpha* is shown in Figure 1. (a) (left panel). A clear excess over the background is apparent around the source direction. The excess is broadly distributed, up to  $\sim 30^\circ$ , due to the deterioration of the pointing resolution, caused by the shrinkage of the gamma-ray shower image. The OFF source distribution was normalized to that of the ON source by the ratio of the number of the events in  $alpha > 40^\circ$  (0.88). An excess of  $298 \pm 52$  events, with a significance of  $5.7 \sigma$  was obtained in the region of  $alpha < 20^\circ$ .

Since the observations were undertaken at large zenith angles,  $\sim 70^\circ$ , we carefully examined the data and the simulations in more detail:

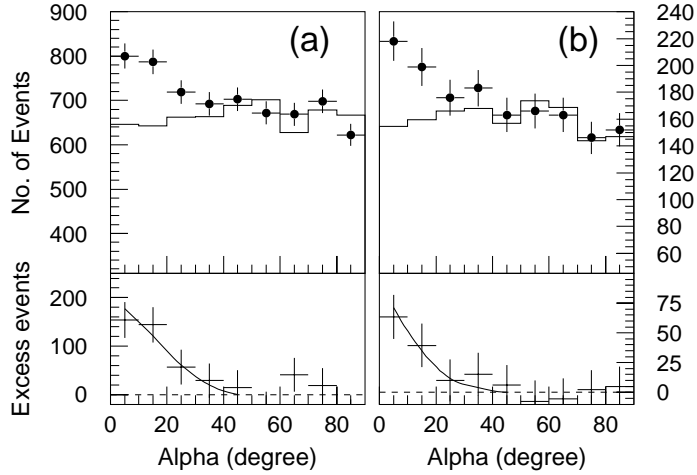


**Fig. 1.** Image orientation angle ( $\alpha$ ) distributions for gamma-ray-like events with respect to the direction to Markarian 421. The left figure (a) shows the distributions for all energies, and the right figure (b) for those with reconstructed energies above 20 TeV. In the upper panel, filled circles with error bars (statistical only) and solid lines are for the ON and OFF source data, respectively. The lower panel shows the excess events of the ON source above the background (OFF source) level. The solid curves show the expected spread of gamma-ray events in the  $\alpha$  distribution from simulations.

1. The imaging parameters of the background events due to cosmic-ray hadrons were compared at large ( $\sim 70^\circ$ ) and small ( $\sim 15^\circ$ ) zenith angles.
2. The *distance* distribution of the gamma-ray selected events was compared to those from simulations.
3. The differential energy spectrum of the Crab nebula was measured at large zenith angles of  $\sim 55^\circ$

These results show the good agreements between data and simulations, therefore we concluded that these consistencies provide robust supporting evidence for the detection of  $E > 10$  TeV gamma-rays from Mrk 421.

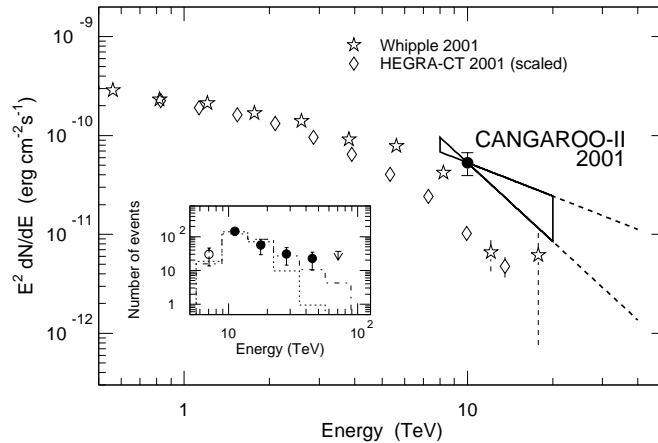
#### 4. Discussion

Figure 2. (inset) shows the raw energy spectrum of the observed gamma-ray events from Mrk 421. The gamma-ray energy was assigned from the pulse-height sum of the individual pixels, which provides an energy resolution of  $\sim 31\%$ . Considering the spill-over effect from the lower energies due to the finite energy resolution, the differential flux was obtained with the assumption of a power-law spectrum,

$$\frac{dN}{dE} = (3.3 \pm 0.9_{stat.} \pm 0.3_{syst.}) \times 10^{-13} \left( \frac{E}{10 \text{ TeV}} \right)^{-(4.0^{+0.9}_{-0.6}{}_{stat.} \pm 0.3_{syst.})} \text{ ph./cm}^2/\text{sec/TeV}$$

with  $\chi^2=2.5/2$  *d.o.f.* The spectral shape was tested with a cutoff spectrum of  $E^{-1.9} \exp(-E/4\text{TeV})$ , as was derived from the measurements by the Whipple and HEGRA-CT groups, with the spectral index being the hardest one observed during the strong flaring period [3] [11]. The fitting result did not improve compared to that with the power-law assumption ( $\chi^2=5.0/3$  *d.o.f.*), as an excess of events above 20 TeV is apparent, as shown in Fig 1. (b). An excess of  $103 \pm 26$  ( $4.0\sigma$ ) was observed with  $\alpha < 20^\circ$ , while 11 events are expected for the cutoff spectrum, based on an estimation using the event ratio between 10–20 TeV and over 20 TeV. However, if a cutoff energy of 8 TeV is assumed, the consistency with the data becomes better (48 events expected for  $E^{-1.9} \exp(-E/8\text{TeV})$ ). This cutoff energy is at the high end of the range allowed for Mrk 501 [1] [2]. Since these two AGNs have similar redshifts, the cutoff energies in both spectra are expected to be similar, assuming the attenuation is predominantly due to infrared absorption. As there is only a  $2\sigma$  difference between our observations and this prediction, our result falls in the acceptable range of the absorption hypothesis due to the cosmic infrared background.

Figure 2. (main panel) shows the measured energy flux, assuming the power-law spectrum. Data for the Whipple [10] and HEGRA-CT groups [3], observed during a similar period of the flaring state (January–March 2001) are also shown. The observation periods were not exactly the same and the source varied significantly during this high state, therefore the absolute fluxes are expected to differ at some level. The absolute flux level determined from the CANGAROO-II data is within the observed range of the flux variation reported by the Whipple group [11], and the spectral slope around 10 TeV is consistent with that of these two groups, supporting the roll-over from the flatter spectrum measured at lower energies.



**Fig. 2.** The observed gamma-ray fluxes (main panel) and the energy spectrum of gamma-ray events (inset). In the inset figure, data are represented by circles with error bars, with a  $2\sigma$  upper limit plotted at the highest energy. Best-fit spectra for a power-law ( $E^{-4.0}$ ; dot-dashed line) and a cut-off ( $E^{-1.9} \exp(-E/4 \text{ TeV})$ ; dotted line) are shown (see text for details). The data shown with the filled circles were used for the spectral shape fitting. In the main panel, the measured flux under the assumption of a power-law spectrum is shown with error bars and the area corresponding to statistical errors of  $\pm 1\sigma$ . Whipple [10] and HEGRA-CT [3] spectra measured in similar periods are also shown. The fluxes plotted for the HEGRA-CT group have been scaled in order to normalize it to the Whipple flux at 1 TeV.

## 5. Conclusions

$E > 10$  TeV gamma-rays from Mrk 421 were detected at a high confidence level at zenith angles of  $\sim 70^\circ$  with 14 hours of observations. The derived spectrum in the region of 10–30 TeV is steeper than that around 1 TeV, which supports the cutoff spectrum of Mrk 421 measured in the 0.2–10 TeV range by other groups. The excess observed above 20 TeV is strongly suggestive of a higher cutoff energy,  $\sim 8$  TeV, compared to the lower energy observations. These observations confirm, with the support of detailed simulations, the viability of the large zenith angle technique.

## References

- [1] Aharonian, F. A. et al. 1999b, A&A 349, 11

- [2] Aharonian, F. A. et al. 2001, *A&A* 366, 62
- [3] Aharonian, F. A. et al. 2002, *A&A* 393, 89
- [4] Börst, H. G., Götting, N & Remillard, R 2001, *IAU Circ.* 7568
- [5] Enomoto, R. et al. 2002a, *Astropart. Phys.* 16, 235
- [6] Enomoto, R. et al. 2002b, *Nature* 416, 823
- [7] Gould, R. J. & Schröder, G. 1967, *Phys. Rev.* 155, 1408
- [8] Nikishov, A. I. 1962, *Sov. Phys. JETP* 14, 393
- [9] Hillas, A. M. 1982, *J. Phys. G* 8, 1475
- [10] Krennrich, F. et al. 2001, *ApJ* 560, L45
- [11] Krennrich, F. et al. 2002, *ApJ* 575, L9
- [12] Li, T. & Ma, Y. 1983, *ApJ* 273, 317
- [13] Okumura, K. et al. 2001, *Proc. 27th Int. Cosmic Ray Conf. (Hamburg)* 7, 2679
- [14] Punch, M. et al. 1992, *Nature* 358, 477
- [15] Punch, M. 1993, Ph.D. thesis, National University of Ireland
- [16] Reynolds, P. T. et al. 1993, *ApJ* 404, 206
- [17] Sommers, P. & Elbert, J.W. 1987, *J. Phys. G: Nucl. Phys.* 13, 553
- [18] Stecker, F. W., de Jager, O.C., Salamon, M.H. 1992, *ApJ* 390, L49
- [19] Tanimori, T. et al. 1994, *ApJ* 429, L61